

EJECTION BEHAVIOR DURING VARIATION OF IMPACT ENERGY AND TARGET WATER SATURATION – THE MEMIN PROJECT. F. D. Sommer¹, F. Reiser¹, A. Dufresne¹, M. H. Poelchau¹, T. Kenkmann¹, and A. Deutsch². ¹Institute for Geoscience, Albert-Ludwigs-Universität Freiburg, D-79104, Freiburg, Germany (Frank.Sommer@geologie.uni-freiburg.de), ²Institute of Planetology, Westfälische Wilhelms-Universität Münster, D-48149 Muenster, Germany.

Introduction. The MEMIN (Multidisciplinary Experimental and Modeling Impact Research Network) project is focused on the formation processes of experimental impact craters into geological materials. The aim of this study is to comprehensively understand the characteristics and the behavior of the material ejected during experimental impact cratering by applying post-mortem analyses in addition to in-situ and real-time measurements, and numerical modeling. A series of mesoscale cratering experiments with different set-ups [1-3] were carried out for examining the influence of projectile mass, velocity, and target water saturation on ejection angle and grain size distribution.

Experimental setup. Steel, iron meteorite (Campo del Cielo IAB) and Al projectiles were accelerated to 2.5-7.8 km/s at the two-stage light-gas gun facilities of the Fraunhofer Institute, Germany. The target (Seeberger sandstone) consists of about 90% quartz and 10% clay minerals; the average grain size is $\sim 100 \mu\text{m}$, and the porosity amounts to $23.1 \pm 0.5 \%$. Ejecta fragments were collected in custom-made catchers of Vaseline and phenolic foam installed parallel to the target surface [4]. Three concentric rings of different colors were painted on the target surface around the point of impact to allow tracing the origin of discrete particles from the target surface to the catcher. The recovered material was investigated with high spatial resolution, and the ejection angles were reconstructed from catcher imprints. For an overview of MEMIN experiments see [3].

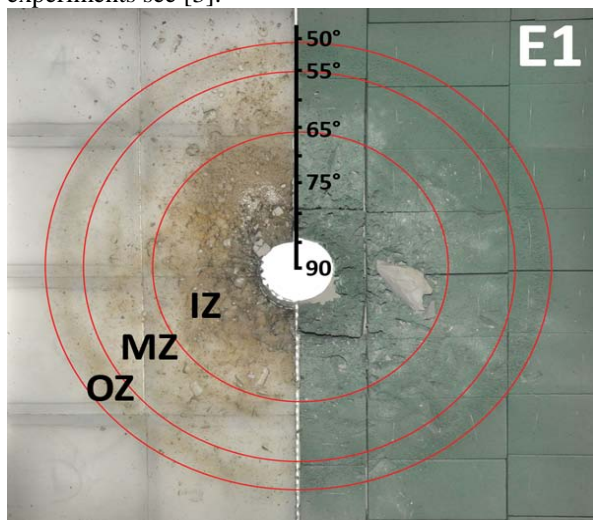


Fig. 1: Ejecta imprint on Vaseline (left) & phenolic foam displaying an outer zone (OZ), inner zone (MZ) an inner zone (IZ); Experiment E1: projectile 7.1g and 4.5km/s on dry target.

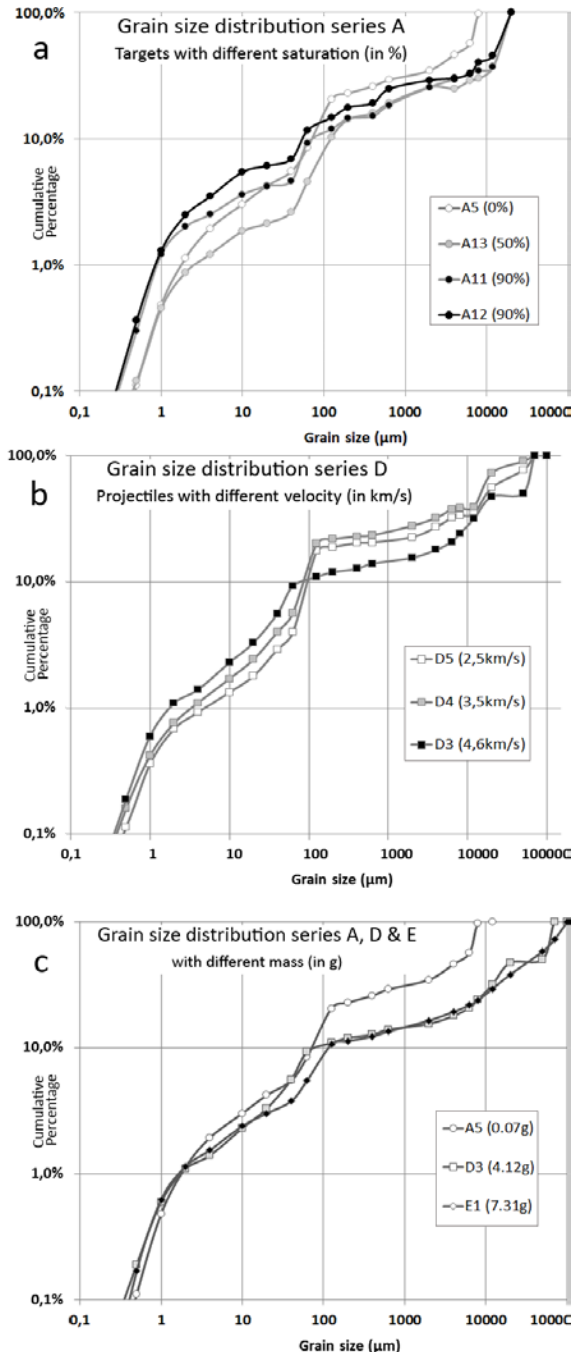


Fig. 2: Grain size distribution under different conditions: a) target saturation, b) projectile velocity, c) projectile mass.

Ejecta distribution. In all experiments, the catchers show three different zones: (i) an outer one, characterized by a ring of fine-grained material; (ii) a middle

zone with only few imprints but a broad range of particle sizes; and (iii) an inner zone containing highly shocked particles and coarse particles, including large spall fragments. According to the imprint density most material impacted here. Particles that originated close to the point of impact preferentially occur in the outer zone while those ejected more distal from the point of impact landed in the middle and inner zones (Fig. 1).

Ejecta angles. For this analysis, the diameter of the outer zone was used to infer the angle of the ejecta cone relative to the target surface. This angle increases from 49° to 62° (i.e., the ejecta cone becomes narrower) with increasing target pore-space saturation, whereas this angle decreases from 56° to 50° with increasing velocity. Ejecta angles (50°) do not change with projectile mass.

Grain size distribution. For particles larger than $63\ \mu\text{m}$, grain size was determined by sieve analysis, and for particles between 0.5 and $200\ \mu\text{m}$ by laser light scattering. In all distribution curves (Fig. 2), particles ranging in size close to the original grain size of the sandstone ($\sim 100\ \mu\text{m}$) form a prominent “hump”, indication common fracturing of the sandstone along grain boundaries. The grain size distribution changes with increasing water saturation of the targets (Fig. 2a) towards a significantly higher amount of fine grained particles ($< 100\ \mu\text{m}$) in ejecta from the 90% water-saturated targets (Fig. 2a). With increasing impact velocity, the fraction of fine grained particles increases and the original grain size has less influence on the grain size distribution (see step at about $100\ \mu\text{m}$ in Fig. 2b). The grain size distribution for the experiments with different projectile mass displays similar profiles, when the difference in total ejected mass is taken into account (experiment A5: 17 g; D3: 1000 g; and E1: 3000 g, Fig. 2c).

Microstructural features. SEM analysis of ejecta particles from the inner zone of the catcher display certain shock features: Kinked and mobilized mica (Figs. 3a-c), shear (Fig. 3c), and conjugate fractures (Fig. 3b) document shock pressures above the Hugoniot elastic limit (3.5 GPa [5]). Particles attached to remnants of the projectile show PDF and SiO_2 melt, substantiating local pressure excursions to over 50 GPa [5,6].

Discussion. Our data allow differentiation of the ejection process into (1) the earliest stage of cratering, in which highly shocked material from close to the impact point is ejected along steep trajectories, forming the inner zone of the ejecta catcher, and to a lesser degree the outer zone; (2) the growth of the excavation flow field with ejection of comminuted material as recorded by the paint tracer analysis. In this phase fine-grained, high-speed material from the proximal area of the impact point hits the outer zone of the catcher; and

(3) unloading of the target, causing ejection of coarse particles and detachment of large spall fragments, both which are implanted in the inner zone of the catcher system. The three stages correspond to observations of the ejecta flow on high-speed videos, where the early ejecta plume is followed by an ejecta cone which, in turn, is replaced by an “ejecta tube” of slow, coarse material and spall pieces in the final stage [2].

Pore-space saturation of sandstone leads to reduced uniaxial compressive strength, thus reducing the impedance mismatch between quartz and pore space and, in turn, the dampening effect porosity has on the shock wave [2,7,8]. It is, however, currently not clear how pore space saturation increases the amount of ejected fine-grained particles ($< 100\ \mu\text{m}$), and which physical process induces the steepening of the ejecta angle.

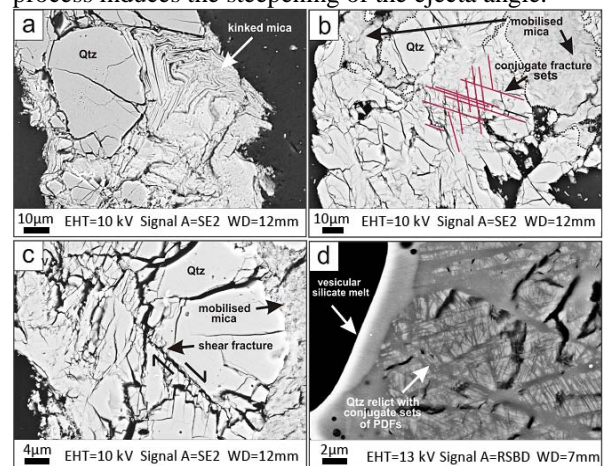


Fig. 2: SEM images of important micro-structural features observed in experimental ejecta fragments.

Our experimental data show that increasing projectile mass does neither change grain size distribution nor ejecta angles. Except for the characteristic peak marking the original grain size of the target sandstone the grain size distribution curves compare well to curves from other cratering experiments [9], and from conventional and atomic explosions [10].

Acknowledgements: This project is funded by the German Research Foundation (DFG), grant FOR-887 and KE 732/16-1.

References: [1] Schaefer F. et al. (2006) *Proc. ESLAB-40*. [2] Kenkmann T. et al. (2011) *MAPS* 46, 890-902. [3] Poelchau M. et al. (2011) *LPS* 42, 1824. [4] Reiser F. et al. (2011) *LPS* 42, 1733. [5] Langenhorst F. & Deutsch A. (2012) *ELEMENTS* 8, 174. [6] Ebert M. et al. (2011) *LPS* 42, 1400. [7] Baldwin E. C. et al. (2007) *MAPS* 42, 1905-1914 [8] Guldemeister N. et al. (2011) *LPS* 42, 1104. [9] Cintala M. J. et al. (1984) *LPS XVI*, 131-132. [10] O’Keefe J.D. & Ahrens T.J. (1985) *Icarus* 62, 328-338.